W.-T. Hsu, J. R. Clark, and C. T.-C. Nguyen, "Mechanically temperature-compensated flexural-mode micromechanical resonators," *Technical Digest*, IEEE Int. Electron Devices Meeting, San Francisco, California, Dec. 11-13, 2000, pp. 399-402.

Mechanically Temperature-Compensated Flexural-Mode Micromechanical Resonators

Wan-Thai Hsu, John R. Clark, and Clark T.-C. Nguyen

Center for Integrated Micro Systems
Department of Electrical Engineering and Computer Science
University of Michigan, Ann Arbor, MI 48109-2122, U.S.A.

ABSTRACT

An IC-compatible, high frequency (HF), lateral micromechanical resonator supported by a mechanical structure designed to introduce stresses that counteract temperature-induced frequency shifts, has been demonstrated at 10 MHz with a much-reduced temperature coefficient of –2.5 ppm/^{o}C and a Q of greater than 10,000. These values constitute substantial improvements over the –17 ppm/^{o}C and 3,000 posted by previous clamped-clamped beam vertical resonators in this frequency range, and represent significant strides towards reducing the thermal dependence of micromechanical resonators, possibly to the point where such devices can be used in on-chip high-Q reference oscillator applications without the need for electronic temperature compensation.

I. INTRODUCTION

Recent demonstrations of 10 MHz clamped-clamped beam vibrating micromechanical ("μmechanical) resonators with Q's on the order of 3,000 [1] have spurred interest in using these devices as high-Q tanks for the low-phase noise reference oscillators needed in communication transceivers and instrumentation. Further incentive for doing this arises from the potential for single-chip integration of such oscillators using a merged transistor/MEMS process technology [2]. However, although the Q of such resonators should be just sufficient to attain the needed phase noise performance in this application, their thermal stability falls well short of needed specifications, typically exhibiting frequency variations on the order of 1760 ppm over a 27^{o}C to 107^{o}C temperature range.

In previous work [3], a geometric stress-compensation design technique was demonstrated on low-frequency (LF, e.g., 80 kHz) nickel folded-beam μmechanical resonators that used a geometrically-tailored stress versus temperature function to cancel the thermal dependence of the material Young's modulus, resulting in an overall lower frequency excursion over a given temperature range, and generating zero temperature coefficient TC_{fo} points in the process. This work now introduces a new stress-tailoring mechanical support structure to extend the above geometric stress-compensation technique to higher frequency (HF) flexural-mode beam resonators more appropriate for use in practical reference oscillator applications. Using this new design, a 10 MHz μmechanical resonator with a Q >10,000—substantially higher than previous ones [1]—is demonstrated with a frequency variation of only 200ppm over a 27^{o}C to 107^{o}C temperature range.

II. TEMPERATURE INSENSITIVE RESONATOR STRUCTURE AND OPERATION

Figure 1 presents the perspective-view schematic of the mechanically temperature-compensated resonator, indicating key components and specifying a preferred bias and excitation configuration. As shown, this structure consists of a flexural-mode resonator beam anchored to the substrate at one end, but supported on the other by a folded structure comprised of a truss section attached to two outer beams. Metal electrodes are positioned on either side of the resonator beam to allow lateral (i.e., x-directed) excitation using the voltage configuration shown, where a DC bias voltage V_P is applied to the conductive beam, and an ac excitation voltage v_i to the input electrode. This combination of voltages across the input electrode-to-resonator gap generates a V_P-multiplied force at the frequency of v_i that drives the beam into vibration when its frequency matches the resonance frequency f_o.

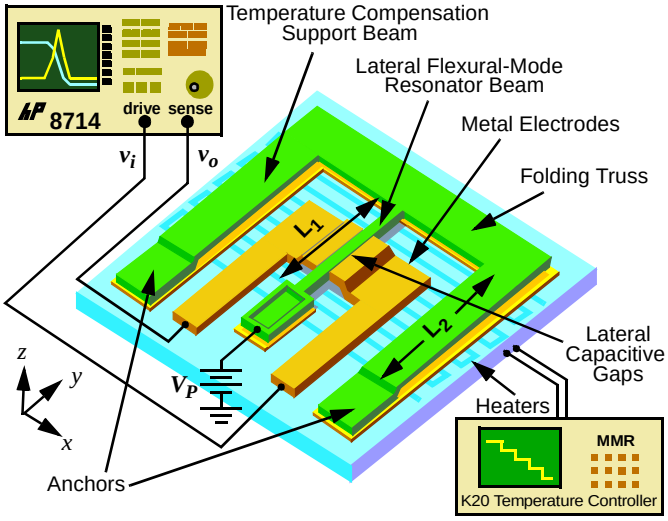

Fig. 1: Perspective-view schematic of a mechanically temperature-compensated micromechanical resonator.

Unlike previous HF vertical resonators (i.e., moving perpendicular to the substrate), which were generally constrained by processing complexity considerations to be one-port devices, the device of Fig. 1 has two-ports. This feature, made possible by lateral operation, not only facilitates the measurement of frequency characteristics for this device by eliminating the need for a bias tee and greatly reducing port-to-port feedthrough, but also simplifies the design of systems using this device, such as oscillators [4] or Q-controlled filters [5].

To insure that only the resonator beam vibrates when excitation signals are applied, the outer support beams are made much wider than the resonator beam, making them rigid against lateral motions. The outer beams are also designed to be longer than the resonator beam, so they will expand faster than it with increasing temperature, generating a net tension in the resonator beam, as shown in the FEM simulation of Fig. 2.

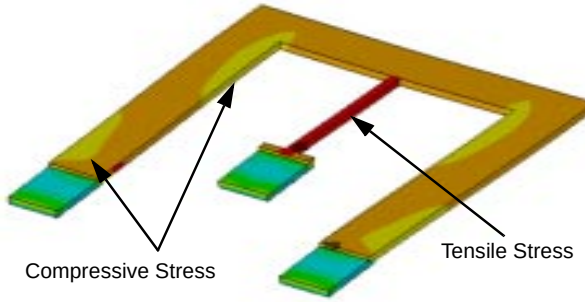

Fig. 2: FEM-simulated Stress distribution on a temperature-insensitive resonator at an elevated temperature.

This tensile stress serves to increase the beam's resonance frequency, and thus, oppose frequency decreases caused by Young's modulus temperature dependence, resulting in a smaller overall f_o excursion over a given temperature range.

In addition to temperature insensitivity, this design also features a support structure that effectively reduces energy radiation into the substrate during resonance vibration. In particular, although one end of the resonator beam is rigidly anchored to the substrate (i.e., a fixed end condition) the other is held relatively softly by the folding truss support system, in what effectively amounts to an end condition that is somewhat more decoupled from the substrate than a directly anchored end condition. This end condition, together with the use of a lateral (rather than a vertical) vibration mode, effectively reduces anchor losses to the substrate, allowing higher resonator Q than previous clamped-clamped beam resonators.

III. TEMPERATURE-INSENSITIVE RESONATOR DESIGN

In the lateral vibration mode, the beam of Fig. 1 essentially has fixed-fixed end conditions, so the expression for its resonance frequency is identical to that of previous clamped-clamped beam resonators [1]. Using Euler-Bernoulli theory, and modeling the thermal dependence of the beam by explicitly expressing stresses due to geometric expansions or contractions as functions of temperature, the expression for resonance frequency can be written as

$$f_o = 1.027\sqrt{\frac{E}{\rho}}\frac{W_1}{L_1^2}\left(1 + 0.293\frac{L_1^2}{EW_1^2}\sigma\right)^{\frac{1}{2}} \quad (1)$$

where L_1 and W_1 are the length and width of the resonator beam, respectively; and E and ρ, are the Young's modulus and density of its structural material, respectively; σ is the longitudinal stress generated by thermal expansion differences between the resonator beam and its compensating suspension network, given by

$$\sigma = E(\alpha_{poly} - \alpha_{sub})\Delta T\left(\frac{L_2}{L_1} - 1\right) \quad (2)$$

where α_{poly} and α_{sub} are the thermal expansion coefficients for the (polysilicon) structural material and the substrate, respectively, and $\Delta T = T\text{-}T_o$ is the temperature T variation from room temperature T_o. From (1) and (2), the temperature coefficient of the resonance frequency TC_{fo} is found to be

Table I: Parameters for Temperature-Insensitive Resonators

Parameters	Value	Units
Resonator Beam Length, L_1	40	μm
Resonator Beam Width, w_1	2	μm
Folding Truss Length, L_f	80	μm
Folding Truss Width, W_f	20	μm
Structural Layer Thickness, t	2.2	μm
Compensation Beam Length, L_2	variable	μm
Compensation Beam Width, W_2	20	μm
Electrode-Resonator Gap Spacing, d	0.1	μm
Electrode Overlap Area	44	μm^2
Nominal Resonance Frequency, f_o	10	MHz
Young's Modulus of Polysilicon, E	1.5e12	$dyne/cm^2$
Temperature Coefficient of E, α_E	–46	$ppm/^oC$
Thermal Expansion Coeff. of Poly-Si, α_{poly}	2.9	$ppm/^oC$
Thermal Expansion Coeff. of Substrate, α_{sub}	2.0	$ppm/^oC$
Density	2.33	g/cm^3

$$TC_{fo} \approx \frac{\alpha_E + \alpha_{poly}}{2} + 0.146\left(\frac{L_1}{W_1}\right)^2(\alpha_{poly} - \alpha_{sub})\left(\frac{L_2}{L_1} - 1\right) \quad (3)$$

where α_E is temperature coefficient of the Young's modulus, and where a dependence on the ratio of the support and resonator beam lengths, L_2/L_1, is clearly seen.

The first term of (3) is merely the TC_{fo} of a clamped-clamped beam, while the second term is generated by action of the compensation structure. From (3), a reduction in the TC_{fo} is possible only if (1) the thermal expansion coefficient of the structural material is different from that of the substrate; and (2) L_2/L_1 is not unity. Moreover, the L_1/W_1 term in (3) can be interpreted as a gain term in the expression, that amplifies or attenuates the compensation effect when L_1 and L_2 are unequal. In high frequency resonators, where L_1/W_1 must be chosen small, larger L_2/L_1 ratios are generally required. Using the formulations above, Table I,summaries the temperature-insensitive resonator design of this work.

IV. FABRICATION

As mentioned in Section II, the key feature of this resonator design that enables improved performance is its use of lateral mode vibrations, which not only facilitates the design of the temperature compensating support structure, but also reduces anchor losses to the substrate (raising its Q), and makes available two input ports (which greatly facilitates circuit design with this device). However, for impedance matching reasons [1], lateral operation at this frequency range also necessitates high aspect-ratio, submicron, lateral electrode-to-resonator gaps.

Achieving such gaps in a lateral direction with the needed aspect-ratios would be a challenging proposition for a conventional surface micromachining process armed with only present-day lithographic and etch capabilities. For this reason, this work utilizes the novel process flow summarized in Fig. 3, that combines surface-micromachining with metal electroplating technology to achieve 1000Å lateral gaps defined by a sidewall sacrificial oxide layer. In this process, a surface micromachining process is first used to achieve polysilicon structures over a bottom sacrificial oxide layer. Another oxide layer is then conformally deposited to form

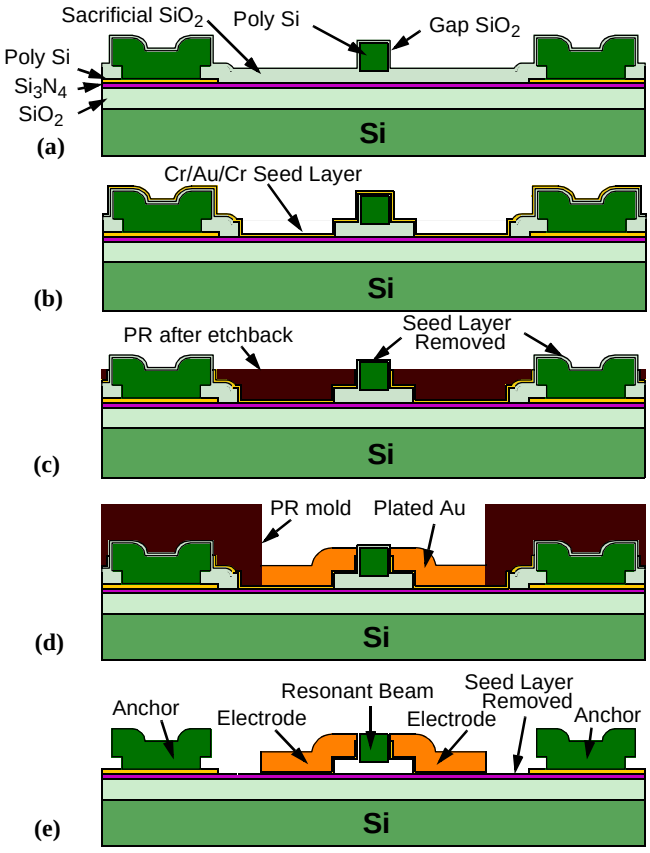

Fig. 3: Process flow of the lateral thin gap process for temperature compensated micromechanical resonators.

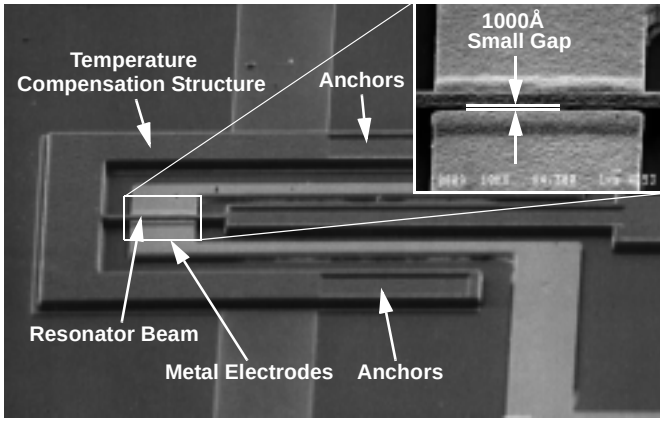

Fig. 4: SEM of a temperature-insensitive micromechanical resonator fabricated using the process of Fig. 3.

sacrificial oxide sidewalls along the resonator beam sides (c.f., Fig. 3(a)). Gold electroplating is then performed through a mold defined by photoresist on one side, and the sidewall oxide on the other, resulting in Au electrodes separated from the resonator sides by only the sidewall oxide thickness (c.f., Fig. 3(d)). A final release step then yields the final cross-section shown in Fig. 3(e) and structures such as shown in the scanning electron micrographs (SEM's) of Fig. 4

V. EXPERIMENTAL RESULTS

Frequency spectra and thermal dependence data were

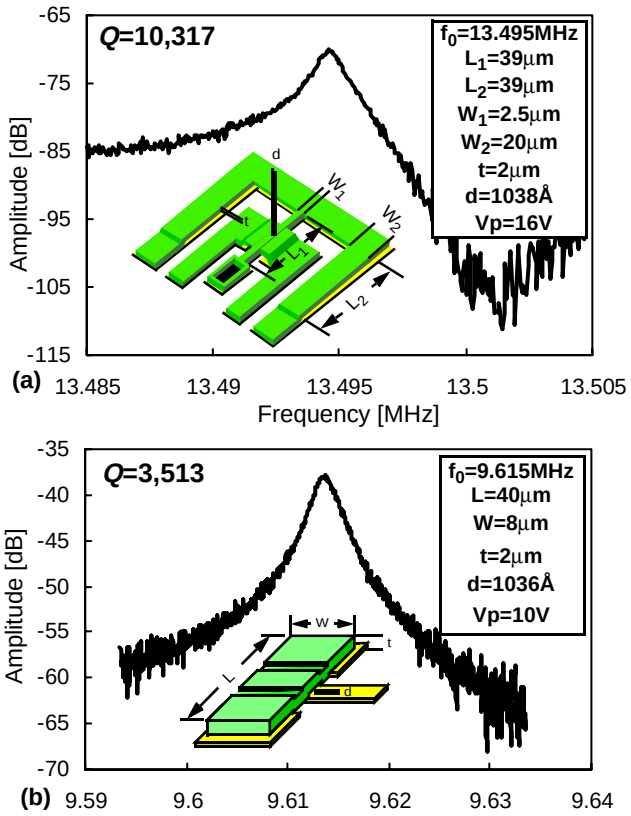

Fig. 5: Measured spectra for (a) a lateral temperature-insensitive resonator (i.e., Fig. 4), and (b) vertical clamped-clamped beam.

obtained using the set-up shown in Fig. 1. Here, an HP 8714C Network Analyzer is used to measure transmission spectra for devices mounted on a printed circuit (PC) board contained within a custom-built vacuum chamber capable of pressures as low as 50 μTorr. The PC board features a special thermally conductive slot to allow mounting of the resonator die on the PC board while also making sufficient thermal contact to an MMR temperature controllable cantilever.

Figure 5 compares measured frequency characteristics for two polysilicon μmechanical resonators: (a) a lateral temperature-insensitive resonator of this work; and (b) a vertical resonator achieved using a conventional surface-μmachining process with an identical polysilicon deposition recipe. As shown, the *Q* of the lateral resonator is almost 3X greater than that of the vertical resonator, most likely indicating better substrate isolation for the former, i.e., smaller anchor losses.

Figure 5 presents a plot of fractional frequency change versus temperature for resonators such as in Fig. 4 with varying L_2/L_1 beam ratios (see Fig. 1). From this plot, control of the resonance frequency temperature dependence can clearly be seen. In particular, for L_2/L_1 beam ratios from 30/40 to 60/40, the temperature coefficient decreases from –35.9 ppm/^{o}C for the L_2/L_1=30μm/40μm device to –2.5 ppm/^{o}C for the L_2/L_1=60μm/40μm device. Unfortunately, however, for higher beam ratios, the temperature coefficient is seen to degrade. A possible mechanism for this is one where the support beams bend upwards or downwards when the stress in the beams becomes too large in devices with large L_2/L_1 beam ratios,

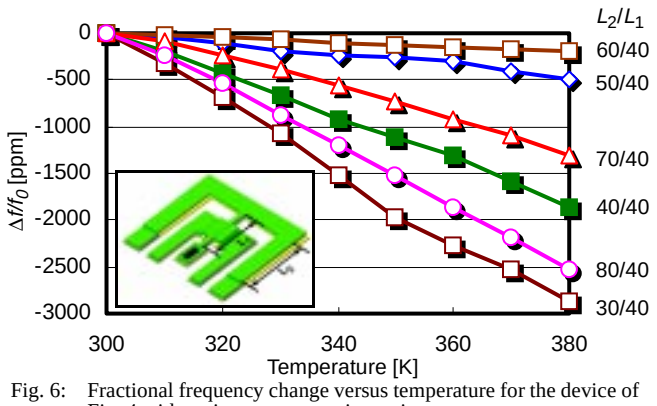

Fig. 6: Fractional frequency change versus temperature for the device of Fig. 4 with various compensation ratios.

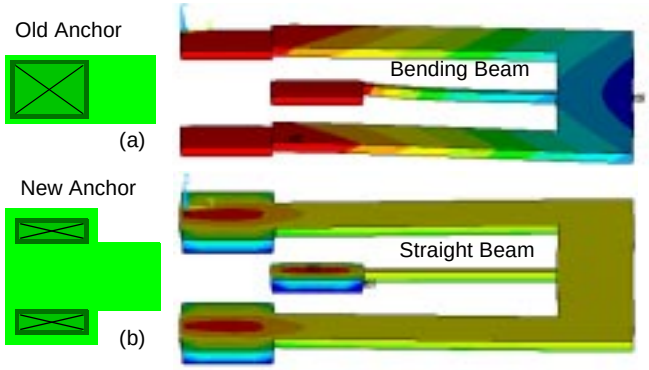

Fig. 7: FEM vertical displacement simulations for (a) conventional anchors and (b) side-anchors. Beam bending is seen in (a).

thereby suppressing and eventually reversing tensile stresses.

That bending occurs in the structure has now been verified via FEM analysis. Figure 7(a) presents the FEM-simulated shape of a temperature-insensitive resonator with the design of Fig. 1 at an elevated temperature of 100°C, clearly showing an upward bending of the beam. However, simulation also shows that this bending occurs even for a cantilever beam with a rigid anchor of the type used in Fig. 7(a). This is immediately understandable upon recognition that in this anchor design, the bottom side of the anchor is attached to the substrate, so it expands or contracts at a different rate than its top side, and this results in downward bending of the beam, as shown in Fig. 7(a). Although, on one hand, this result seems to lend credence to a bending-based mechanism for the observed back-and-forth TC_{fo} behavior of Fig. 6, on the other hand, it raises questions as to whether or not the mechanism behind the initial lowering of the TC_{fo} is really as described in Section II. In other words, does TC_{fo} control occur due to thermal expansion differences that induce stress directly in the beam, or does control actually arise less directly, from expansion differences that induce stresses to cause beam bending.

Pursuant to answering this question, a second fabrication run was done that included structures using a modified anchor design that eliminates the beam bending mechanism described above. This new anchor, shown in Fig. 7(b), redirects top-to-bottom side expansion differences so that they occur only in a direction orthogonal to the length of the resonator (or support) beam, thus, eliminating beam bending along the length of the beam. Figure 8 presents the SEM of a 10 MHz version of a temperature-insensitive resonator using these new anchors. The inset of Fig. 8 presents the fractional frequency versus temperature curve for this resonator, again for various values of L_2/L_1, showing clearly that without bending, there is very little control over the frequency versus temperature curve. This suggests that the difference in the thermal expansion coefficients of substrate silicon and polysilicon is large enough to cause beam bending, but not large enough to generate enough direct beam stress to alter its TC_{fo}.

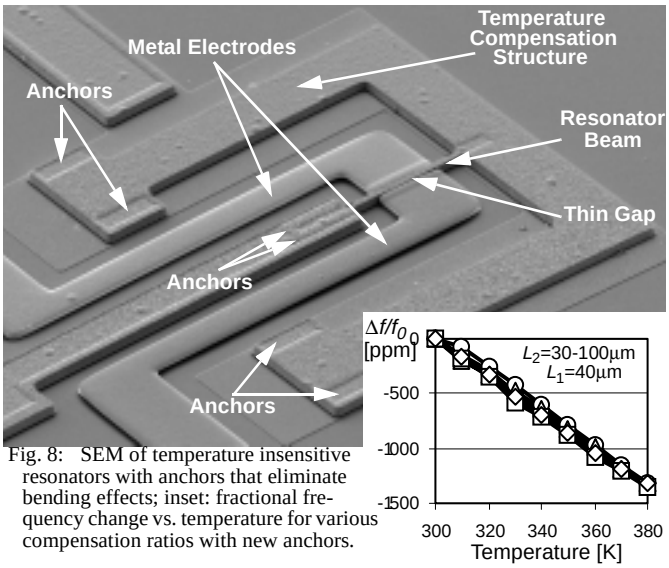

Fig. 8: SEM of temperature insensitive resonators with anchors that eliminate bending effects; inset: fractional frequency change vs. temperature for various compensation ratios with new anchors.

Next generation structures are presently underway that use different materials for the resonator and stress-controlling suspension beams to insure the *direct* generation of sufficient stresses.

VI. CONCLUSIONS

Using a new geometric stress-compensating support structure together with a process technology that achieves submicron lateral electrode-to-resonator gaps, micromechanical resonators at HF frequencies have been demonstrated with both higher *Q*'s and lower temperature coefficients than previous clamped-clamped beam resonators in this frequency range. Although in this work the mechanism for temperature compensation may not have been as direct as originally expected by design (due to beam bending effects), the concept of using a geometrically-tailored stress versus temperature function to compensate for Young's modulus thermal dependence still applied, and should prove instrumental in future resonator designs targeted for communications and timekeeper applications.

***Acknowledgment*:** This work was supported under DARPA Cooperative Agmt. No. F30602-97-2-0101.

References:

[1] F. Bannon, *et al.*, *IEEE JSSC*, pp. 512-526, April 2000.
[2] J. H. Smith, *et al.*, *IEDM'95*, pp. 609-612.
[3] W.-T. Hsu, *et al.*, *Ultras. Symp.'98*, pp. 945-948.
[4] C. Nguyen, *et al.*, *IEEE JSSC*, pp. 440-445, April 1999.
[5] K. Wang, *et al.*, *IEEE JMEMS*, pp. 534-557, Dec. 1999.